Available online at www.sciencedirect.com
ScienceDirect
Journal of Power Sources 164 (2007) 590–605
JOURNAL OF POWER SOURCES
www.elsevier.com/locate/jpowsour

Water equilibria and management using a two-volume model of a polymer electrolyte fuel cell

Amey Y. Karnik [a,*], Anna G. Stefanopoulou [a], Jing Sun [b]

[a] *Department of Mechanical Engineering, University of Michigan, United States*
[b] *Naval Architecture and Marine Engineering Dept., University of Michigan, United States*

Received 24 August 2006; received in revised form 16 October 2006; accepted 16 October 2006
Available online 15 December 2006

Abstract

In this paper, we introduce a modified interpretation of the water activity presented in Springer et al. [T.E. Springer, T.A. Zawodzinski, S. Gottesfeld, Polymer electrolyte fuel cell model, J. Electrochem. Soc. 138 (8) (1991) 2334–2342]. The modification directly affects the membrane water transport between the anode and the cathode (two electrodes) of the polymer electrolyte membrane (PEM) fuel cell in the presence of liquid water inside the stack. The modification permits calibration of a zero-dimensional isothermal model to predict the flooding and drying conditions in the two electrodes observed at various current levels [D. Spernjak, S. Advani, A.K. Prasad, Experimental investigation of liquid water formation and transport in a transparent single-serpentine PEM fuel cell, in: Proceedings of the Fourth International Conference on Fuel Cell Science, Engineering and Technology (FUELCELL2006-97271), June 2006]. Using this model the equilibria of the lumped water mass in the two electrodes are analyzed at various flow conditions of the stack to determine stable and unstable (liquid water growth) operating conditions. Two case studies of water management through modification of cathode inlet humidification and anode water removal are then evaluated using this model. The desired anode water removal and the desired cathode inlet humidification are specified based upon (i) the water balance requirements, (ii) the desired conditions in the electrodes, and (iii) the maximum membrane transport at those conditions.

Keywords: PEMFC; Water management; Anode water removal; Water dynamics

1. Introduction

Due to the significant influence of water [3,4] on the performance of the polymer electrolyte membrane fuel cell (PEMFC), many models have been developed to capture its spatial distribution within a fuel cell stack. These computational fluid dynamics (CFD) models are then used to optimize the cell flow field (width, length, orientation, etc.) and materials (hydrophobicity, porosity, thickness, etc.). Once the optimum fuel cell is designed, CFD models [5] can again, theoretically, be used to select the right number of cells to be combined in a stack in order to avoid large cell-to-cell variations. Although the above fuel cell design process is visionary, it is still far from being realized. Ultra large-scale models [6] have so far been used to simulate medium size single cells with fixed geometry and materials interconnection.

Once the fuel cell is designed the only remaining degrees of freedom for water management are the mass flow rates entering and leaving the electrodes of the fuel cell stack. The actuating mechanisms for controlling water flow rates, for example, anode and cathode inlet humidification, oxygen excess ratio (OER), and anode recirculation, are not spatially distributed, but allow control only in the stack manifolding, which in turn constitutes the boundary control to the electrodes. Water management of the fuel cell stack with these actuators cannot be used to control the spatial distribution of water in the stack (from cell to cell and within the stack material). Nevertheless, one can start by controlling the mass of water in the two lumped volumes that correspond to the anode and the cathode electrodes and augment this methodology with diagnostic mechanisms that detect maldistribution of water through cell to cell variability or large pressure variations [7]. It is through the water management in the electrodes that we hope to control the humidity conditions at the catalyst where the reaction happens.

In this paper, the capabilities of physically actuated system variables to achieve water balance in the stack are evaluated

* Corresponding author. Tel.: +1 734 730 4644; fax: +1 734 730 4644.
E-mail address: akarnik@umich.edu (A.Y. Karnik).

0378-7753/$ – see front matter © 2006 Published by Elsevier B.V.
doi:10.1016/j.jpowsour.2006.10.053

Nomenclature

p	pressure (Pa)
m	mass (kg)
y	vapor mass fraction
W	flow rate (kg s^{-1})
T	temperature (K)
I_{st}	stack Current (A)
N	molar flux (mole s^{-1} cm^{-2})
$\bar{M}$	molecular weight (kg mole^{-1})
R	gas constant (J kg^{-1} K^{-1})
λ	water content
a_w	water activity
ϕ	relative humidity
ω	humidity ratio
$\tilde{k}$	flow coefficient (kg s^{-1} Pa^{-1})

Superscripts and subscripts

a	anode
c	cathode
m	membrane
st	stack
v	vapor phase
l	liquid phase
H_2O	water
H_2	hydrogen
O_2	oxygen
N_2	nitrogen
gen	generated
rem	water removed
in	inlet
out	outlet
sat	saturated

using a zero-dimensional, isothermal, lumped parameter PEMFC stack model similar to [8]. In this low order model, water (both liquid and vapor) accumulates in the lumped volumes of the two electrodes. Additional components in the stack that can potentially store water, such as gas diffusion layer (GDL) and membrane, are neglected. Moreover, the model assumes instantaneous transition from vapor to liquid phase if the partial pressure of water vapor exceeds the saturation pressure. Finally, an ideal thermal control is assumed that maintains constant temperature throughout the stack.

Clearly, the stack model with these assumptions will not capture any spatial distribution. Instead, this low order model focuses on important lumped phenomena, such as, anode flooding at lower current densities [2,9] and anode drying at higher current densities [10]. In order to capture the phenomenon of anode flooding, the model presented in [12,11] is modified to allow liquid water on the cathode side of the membrane to influence membrane water transport.

The low order model facilitates the stability analysis of the water equilibria arising from employing various popular water management techniques, such as controlling humidity of inlet flow or anode water removal using recirculation [14,13]. This step is important since only stable equilibria can be achieved via feedforward maps (look-up tables) that use the information of the current drawn to determine, for instance, the appropriate level of anode water removal [15] or cathode inlet humidification [16,17].

We demonstrate a methodology to achieve water management using (i) cathode inlet humidification, and (ii) anode water removal, as actuating mechanisms. Other mechanisms, namely, anode humidification and cathode water removal through high oxygen excess ratio, might be necessary when operating at very low or very high currents. The use of these mechanisms will need more investigation than the one that can be allotted in this paper.

The paper is structured as follows: the stack model related to water management is discussed in Section 2. The water dynamics in the anode and the cathode and their interaction under different operating conditions are discussed in Section 3. The model predictions of stack flooding and drying characteristics without active water management are discussed in Section 4. In Section 5, different water management strategies involving cathode inlet humidification and anode water removal are identified and their ability to achieve particular water conditions are investigated independently of specific actuating components. Section 6 summarizes the results in the paper.

2. Model for water management analysis

In this section, we first present the membrane water transport model [1] with a modification to the typical interpretation of water activity used in [11,12,18]. The proposed modification enables the prediction of liquid water accumulation in the anode at low current densities, which is important for mobile fuel cell applications due to the frequent operation at low loads. Then, we integrate this modified membrane water transport model with anode and cathode mass balance equations to develop the two-volume fuel cell model.

2.1. Membrane water transport

The water transport through the membrane from the anode to the cathode, W_{memb}, is given by

$$W_{memb} = \bar{M}_{H_2O} A_{fc} n_{cells} (N_{drag} - N_{diff}), \quad (1)$$

where A_{fc}(cm^2) denotes the active fuel cell area, n_{cells} the number of cells in the stack and $\bar{M}_{H_2O}$ the molecular weight of water. The molar flux per unit cell from the anode to the cathode due to the electro-osmotic drag is N_{drag} (mole s^{-1} cm^{-2}), while N_{diff} (mole s^{-1} cm^{-2}) is the molar flux per unit cell from the cathode to the anode due to the difference in water concentration on the anode and cathode sides.

These fluxes depend upon the stack current, I_{st}; the membrane water content, λ_m; and the amount of water present on the anode and cathode sides [1,11]. The molar flux due to electro-osmotic

drag from anode to cathode, N_{drag}, is given by [1]

$$N_{drag} = n_d \frac{I_{st}}{A_{fc} F}, \tag{2}$$

with

$$n_d = 0.0029\lambda_m^2 + 0.05\lambda_m - 3.4 \times 10^{-19},$$

where F is Faraday's constant.

The molar flux due to back diffusion from cathode to anode, N_{diff}, is modeled as [1]

$$N_{diff} = \alpha_D D_w \frac{\rho_{m,dry}}{t_m \bar{M}_{m,dry}} (\lambda_c - \lambda_a), \tag{3}$$

with

$$D_w = D_\lambda \exp\left(2416\left(\frac{1}{303} - \frac{1}{T_{st}}\right)\right),$$

where T_{st} is the stack temperature, t_m is the membrane thickness, $\rho_{m,dry}$ and $\bar{M}_{m,dry}$ are the density and the weight per mole, respectively, of the membrane when dry. The diffusion coefficient, D_w, is scaled using a multiplicative term α_D to serve as a tuning parameter. In our analysis we use α_D in evaluating the effect of membranes with different diffusion properties.[1] The coefficient, D_λ, is defined in [12,11] as

$$D_\lambda = \begin{cases} 10^{-6} & \text{if } \lambda_m < 2 \\ 10^{-6}(1 + 2(\lambda_m - 2)) & \text{if } 2 \le \lambda_m \le 3 \\ 10^{-6}(3 - 1.67(\lambda_m - 3)) & \text{if } 3 < \lambda_m < 4.5 \\ 1.25 \times 10^{-6} & \text{if } \lambda_m \ge 4.5. \end{cases} \tag{4}$$

In the above equations, λ_c and λ_a are the water contents at the cathode and anode side of the membrane, respectively. Water content [1,19] is defined as

$$\lambda_{(\cdot)} = f_\lambda(a_{w,(\cdot)}), \tag{5}$$

where $a_{w,(\cdot)}$ represents the water activity and the function, f_λ is shown in Fig. 1. Here, subscript "(·)" is to be replaced with "a", "c" and "m" for anode, cathode and membrane, respectively.

Two important characteristics of the relation between $a_{w,(\cdot)}$ and $\lambda_{(\cdot)}$ are that it is monotonic and has an upper bound. The upper bound on the membrane water content, λ_{max}, corresponds to the water content of the membrane when completely immersed in liquid water [1]. In this analysis, this maximum water content is achieved once the water activity equals 3, beyond which the water content is constant [19].

The average membrane water activity, $a_{w,m}$, is defined[2] as

$$a_{w,m} = \frac{a_{w,a} + a_{w,c}}{2}, \tag{6}$$

where $a_{w,a}$ and $a_{w,c}$ correspond to the water activities on anode and cathode sides of the membrane, respectively.

[1] The term α_D can also be combined with D_λ, thereby making D_λ as the tuning parameter.

[2] Note that in the following work $a_{w,m}$ is defined as the average membrane water activity, similar to [12]. Other possible definitions that could be employed [20] are $a_{w,m} = a_{w,a}$ to reflect the importance of the anode side water activity, or $a_{w,m} = \min(a_{w,a}, a_{w,c})$ to capture the conditions of the limiting electrode.

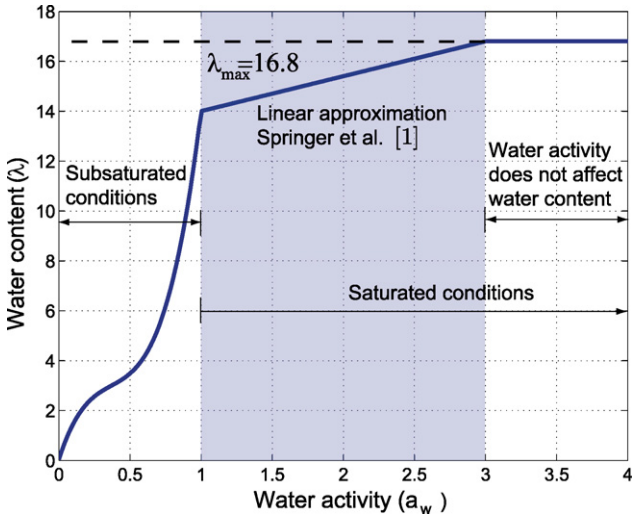

Fig. 1. Water content as a function of water activity.

In this simplified isothermal model, the water activity on the anode or the cathode sides of the membrane is defined as

$$a_{w,(\cdot)} = \frac{m_{H_2O,(\cdot)}}{m^{sat}_{H_2O,v,(\cdot)}}, \tag{7}$$

where $m_{H_2O,(\cdot)}$ is the total water in the adjacent electrode (anode or cathode). The maximum water vapor that can be present in that electrode, $m^{sat}_{H_2O,v,(\cdot)}$, is given by

$$m^{sat}_{H_2O,v,(\cdot)} = \frac{p_{sat}\left(T_{(\cdot)}\right) \tilde{V}_{(\cdot)}}{R_{H_2O} T_{(\cdot)}}, \tag{8}$$

where $p_{sat}(T_{(\cdot)})$ denotes the saturation pressure corresponding to temperature $T_{(\cdot)}$, where $T_{(\cdot)}$ is the temperature, $\tilde{V}_{(\cdot)}$ is the lumped volume of the electrode and R_{H_2O} is the gas constant of water vapor.

With $a_{w,(\cdot)}$ defined as Eq. (7), W_{memb} is influenced by liquid water in the stack and the isothermal stack model equations used here can capture anode flooding behavior under conditions experimentally observed [21,2], when the diffusion coefficient, α_D, is appropriately tuned or defined. Different modifications can be found in literature [19,22] that incorporate effect of liquid water on membrane water transport, however, these are applicable to more detailed models.

Note here that, modeling $a_{w,(\cdot)}$ to be equal to the relative humidity in the adjacent electrode, $\phi_{(\cdot)}$, as in [18,11,12], instead of Eq. (7), always results in sub-saturated anode conditions even when the cathode is flooded. Indeed, if

$$a_{w,(\cdot)} = \phi_{(\cdot)} = \frac{p_{H_2O,v,(\cdot)}}{p_{sat}(T_{(\cdot)})}, \tag{9}$$

where $p_{H_2O,v,(\cdot)}$ is the partial pressure of water vapor in an electrode, then the water activity is always less than 1, as $p_{H_2O,v,(\cdot)} \le p_{sat}(T_{(\cdot)})$. Even when liquid water is present on the cathode side, using the activity definition (9), we have $a_{w,c} = 1$. With the maximum water activity in the cathode being 1, the water transported from cathode to anode is limited and can at most cause saturating condition in the anode. Specifically, when the partial pressure of water vapor in anode reaches saturation, $a_{w,a} = 1$, the water transport from cathode to anode stops be-

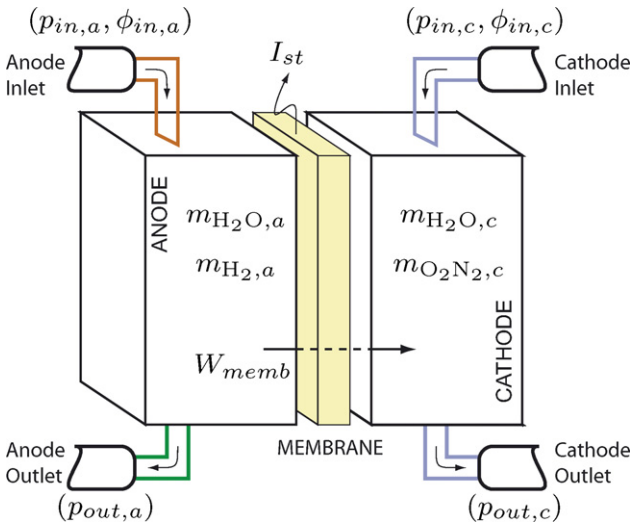

Fig. 2. Lumped volumes representing the two electrodes of the fuel cell stack.

cause the diffusion requires a positive gradient in water content between anode and cathode, that is, $\lambda_a < \lambda_c$. This implies that an isothermal stack model using water activity definition (9) will never exhibit anode flooding.

The model for water mass transport through the membrane is next used in the mass conservation equations applied to the lumped volumes of the anode and cathode electrodes of the fuel cell. The resulting ordinary differential equations are then used to find the mass equilibria and stability properties for the dry gas and the water inside the two electrodes.

2.2. Mass conservation

The fuel cell stack equilibria are derived by assuming isothermal conditions in the electrodes and using mass conservation for the important species shown in Fig. 2, namely, the water in the anode and the cathode, $m_{H_2O,a}$ and $m_{H_2O,c}$, respectively, the hydrogen in the anode, $m_{H_2,a}$, and dry air in the cathode, $m_{O_2N_2,c}$. The water mass in the two electrodes are given by [12]

$$\frac{dm_{H_2O,a}}{dt} = W_{H_2O,in,a} - W_{H_2O,out,a} - W_{memb} \tag{10}$$

$$\frac{dm_{H_2O,c}}{dt} = W_{H_2O,gen} + W_{H_2O,in,c} - W_{H_2O,out,c} + W_{memb}, \tag{11}$$

where $W_{H_2O,in,a}$ and $W_{H_2O,out,a}$ are the mass flow rates of water entering and leaving the anode, respectively. Similarly, $W_{H_2O,in,c}$ and $W_{H_2O,out,c}$ are the mass flow rates of water entering and leaving the cathode. The water generation rate due to the electrochemical reaction is given by

$$W_{H_2O,gen} = n_{cells}\frac{I_{st}}{2F}\bar{M}_{H_2O}. \tag{12}$$

The mass flows in the two electrodes can be derived through generic equations, where "(·)" should be replaced by "a" for anode and "c" for cathode. The mass of water entering an electrode is given by

$$W_{H_2O,in,(\cdot)} = y_{v,in,(\cdot)}W_{in,(\cdot)} \tag{13}$$

$$W_{in,(\cdot)} = \tilde{k}_{in,(\cdot)}(p_{in,(\cdot)} - p_{(\cdot)}), \tag{14}$$

where $y_{v,in,(\cdot)}$ is the mass fraction of water vapor in the inlet flow. The total flow entering an electrode, $W_{in,(\cdot)}$, is modeled using a linear flow model with a flow coefficient $\tilde{k}_{in,(\cdot)}$. Here, $p_{in,(\cdot)}$ is the total pressure at the electrode inlet while $p_{(\cdot)}$ is the total pressure within the electrode.

The mass fraction of water vapor in the inlet flow is

$$y_{v,in,(\cdot)} = \frac{p_{H_2O,v,in,(\cdot)}\bar{M}_{H_2O}}{p_{H_2O,v,in,(\cdot)}\bar{M}_{H_2O} + \left(p_{in,(\cdot)} - p_{H_2O,v,in,(\cdot)}\right)\bar{M}_{g,(\cdot)}}, \tag{15}$$

with the partial pressure of vapor at the electrode inlet as

$$p_{H_2O,v,in,(\cdot)} = \phi_{in,(\cdot)}p_{sat}(T_{in,(\cdot)}), \tag{16}$$

where $p_{sat}(T_{in,(\cdot)})$ denotes the saturation pressure corresponding to inlet temperature $T_{in,(\cdot)}$, and $\phi_{in,(\cdot)}$ is the relative humidity of the inlet flow. Here, we assume that no liquid water is supplied to the electrodes.

Meanwhile, $\bar{M}$ is used to represent molecular weight and the subscript "g, (·)" denotes the dry gas reactant in the electrode, and hence, is replaced by "H_2" for hydrogen in anode and "O_2N_2" for dry air in the cathode.

Using Dalton's law of partial pressures, the total pressure in an electrode is given by

$$p_{(\cdot)} = p_{H_2O,v,(\cdot)} + p_{g,(\cdot)}, \tag{17}$$

where $p_{g,(\cdot)}$ and $p_{H_2O,v,(\cdot)}$ are the partial pressures of the dry gas and the water vapor in the electrode.

Considering the ideal gas law, $p_{H_2O,v,(\cdot)}$ depends upon the mass of water vapor in the electrode, $m_{H_2O,v,(\cdot)}$, as

$$p_{H_2O,v,(\cdot)} = \frac{R_{H_2O}T_{(\cdot)}}{\tilde{V}_{(\cdot)}}m_{H_2O,v,(\cdot)}. \tag{18}$$

Assuming instantaneous condensation and evaporation of water, the mass of water vapor is given by

$$m_{H_2O,v,(\cdot)} = \min\left\{m_{H_2O,(\cdot)}, m^{sat}_{H_2O,v,(\cdot)}\right\}, \tag{19}$$

where $m^{sat}_{H_2O,v,(\cdot)}$ is the maximum water vapor that can be present in the electrode (see Eq. (8)).

The partial pressure of dry gas, $p_{g,(\cdot)}$, is obtained from the mass of the dry gas in the electrode, $m_{g,(\cdot)}$, using the ideal gas law, as

$$p_{g,(\cdot)} = \frac{R_{g,(\cdot)}T_{(\cdot)}}{\tilde{V}_{(\cdot)}}m_{g,(\cdot)}, \tag{20}$$

where $R_{g,(\cdot)}$ represents the gas constant for the dry gas in the electrode.

The water leaving an electrode is separated into liquid and vapor phases due to differences in their flow properties.

$$W_{H_2O,out,(\cdot)} = W_{H_2O,v,out,(\cdot)} + W_{H_2O,l,out,(\cdot)}, \tag{21}$$

where $W_{H_2O,v,out,(\cdot)}$ and $W_{H_2O,l,out,(\cdot)}$ are the flow rates of water vapor and liquid, respectively, leaving the electrode.

The flow rate of water vapor flowing out of an electrode is given by

$$W_{H_2O,v,out,(\cdot)} = y_{v,(\cdot)} W_{out,(\cdot)} \quad (22)$$

$$W_{out,(\cdot)} = \tilde{k}_{out,(\cdot)}(p_{(\cdot)} - p_{out,(\cdot)}), \quad (23)$$

where $p_{out,(\cdot)}$ is the pressure at the electrode outlet, $W_{out,(\cdot)}$ is the net mass flow rate of the gases leaving the electrode, and $\tilde{k}_{out,(\cdot)}$ is the linear flow coefficient for outlet flow. The mass fraction of water vapor in an electrode is

$$y_{v,(\cdot)} = \frac{m_{H_2O,v,(\cdot)}}{m_{H_2O,v,(\cdot)} + m_{g,(\cdot)}}. \quad (24)$$

Based on [23], the flow rate of liquid water drained out of an electrode, $W_{H_2O,l,out,(\cdot)}$, depends upon the accumulated mass of liquid water and the pressure drop across the electrode as

$$W_{H_2O,l,out,(\cdot)} = (p_{(\cdot)} - p_{out,(\cdot)})\bar{f}(m_{H_2O,l,(\cdot)}), \quad (25)$$

where function $\bar{f}(m_{H_2O,l,(\cdot)})$ depends upon channel geometry and material properties. The mass of liquid water accumulated in the electrode, $m_{H_2O,l,(\cdot)}$, is given by

$$m_{H_2O,l,(\cdot)} = m_{H_2O,(\cdot)} - m_{H_2O,v,(\cdot)}. \quad (26)$$

In order to complete the stack model, we need to provide the mass of dry gas in the anode and cathode electrodes. The dynamics of mass of hydrogen in the anode, $m_{H_2,a}$, are modeled by applying conservation of mass, as

$$\frac{dm_{H_2,a}}{dt} = W_{H_2,in,a} - W_{H_2,out,a} - W_{H_2,rct}, \quad (27)$$

where $W_{H_2,in,a}$ and $W_{H_2,out,a}$ are the flow rates of hydrogen at anode inlet and outlet, respectively. The rate at which hydrogen is consumed in the electrochemical reaction is given by

$$W_{H_2,rct} = n_{cells}\frac{I_{st}}{2F}\bar{M}_{H_2}. \quad (28)$$

Similarly, the dynamics of mass of dry air in the cathode are given by

$$\frac{dm_{O_2N_2,c}}{dt} = W_{O_2N_2,in,c} - W_{O_2N_2,out,c} - W_{O_2,rct}, \quad (29)$$

where $W_{O_2N_2,in,c}$ and $W_{O_2N_2,out,c}$ are the flow rates of dry air at cathode inlet and exit, respectively, and the rate at which oxygen is consumed in the electrochemical reaction is given by

$$W_{O_2,rct} = n_{cells}\frac{I_{st}}{4F}\bar{M}_{O_2}, \quad (30)$$

where $\bar{M}_{O_2}$ is the molecular weight of oxygen.

The flow rates of dry gas into and out of the electrode are given by

$$W_{g,in,(\cdot)} = (1 - y_{v,in,(\cdot)})W_{in,(\cdot)} \quad (31)$$

$$W_{g,out,(\cdot)} = (1 - y_{v,(\cdot)})W_{out,(\cdot)}, \quad (32)$$

where $y_{v,in,(\cdot)}$ and $y_{v,out,(\cdot)}$ are the vapor mass fractions in the inlet and exit flows, $W_{in,(\cdot)}$ and $W_{out,(\cdot)}$, respectively.

Oxygen and nitrogen in the cathode are not modeled separately, since we are interested only in the total pressure and water dynamics in the electrode. These dynamics depend upon the molecular weight of the gas mixture which is assumed constant at 29×10^{-3} kg mole^{-1}. Even though oxygen is consumed inside the cathode, this assumption introduces, at the most, a 4% modeling error in the molecular weight of the gas mixture, as the molecular weight of the gas mixture is bounded between 28×10^{-3} and 29×10^{-3} kg mole^{-1}.

Eqs. (10), (11), (27) and (29) obtained through mass conservation are used by the two-volume model to predict the mass equilibria in the lumped volumes of the two electrodes. In these equations, the electrode inlet conditions, that is, inlet pressures $p_{in,a}$ and $p_{in,c}$, and inlet humidities $\phi_{in,a}$ and $\phi_{in,c}$, modify the flows into the two electrodes. Meanwhile, the flows out of the electrodes are affected by the electrode exit conditions $p_{out,a}$ and $p_{out,c}$. The different inputs and dynamic states of the two-volume model can be summarized using Fig. 2.

We show next a stability analysis of different water mass equilibria predicted by this simple two-volume model (Section 3). In Section 4, we state the model predictions of flooding and drying conditions along with a discussion of its key calibrating parameters and we show how the model predications can be used to analyze the suitability of water management schemes.

3. Analysis of equilibrium conditions related to water management

This simplified model can describe complex phenomena associated with the water mass in the stack. For example, consider the case when the inlet and exit conditions of the stack are chosen such that the system is at an equilibrium. If this equilibrium condition is unstable, then in the absence of a proper water management scheme a small change in the stack current can lead to an unbounded growth in the mass of water inside the stack, as shown in Fig. 3.

As time progresses the mass of water in the cathode reaches a level such that the cathode water activity exceeds 3, seen in Fig. 3 at 10 s. Once this condition is reached, the additional water accumulating in the cathode does not increase the back diffusion from cathode to anode, thereby allowing the mass of anode water to equilibrate at a value depending upon the anode inlet and exit flows and the electro-osmotic drag. Thus, Fig. 3 reflects the different stability properties of the anode and cathode water, in presence of a disturbance from stack current.

In this section, equilibrium conditions at which the mass of water in the anode or cathode can exhibit an unstable behavior are identified. First, physical reasoning is used to justify the dynamic behaviors at different operating conditions. Then, a linearized approximation of system dynamics is used to verify the results analytically.

3.1. Stability of different operating conditions

Stability of typical operating points corresponding to different conditions are listed in Table 1. The columns (a) and (b) address the effect of liquid water removal on the stability of the water dynamics in the system. In each case, the behavior of mass of water in anode and cathode is specified separately.

Table 1
Stability of the water dynamics under different operating conditions

Case	Water level		Stable equilibria*			
	$\frac{m_{H_2O,c}}{m^{sat}_{H_2O,v,c}}$	$\frac{m_{H_2O,a}}{m^{sat}_{H_2O,v,a}}$	(a) $\frac{\partial W_{H_2O,l,out,(\cdot)}}{\partial m_{H_2O,l,(\cdot)}} \equiv 0$		(b) $\frac{\partial W_{H_2O,l,out,(\cdot)}}{\partial m_{H_2O,l,(\cdot)}} > 0$	
			Cathode	Anode	Cathode	Anode
(i)	[0 1]	[0 $a_{w,c}$]	Yes	Yes	Yes	Yes
(ii)	[1 3]	[0 1]	Yes	Yes	Yes	Yes
(iii)	[1 3]	[1 $a_{w,c}$]	No	No	Yes	Yes
(iv)	> 3	[0 1]	No	Yes	Yes	Yes
(v)	> 3	[1 3]	No	Yes	Yes	Yes

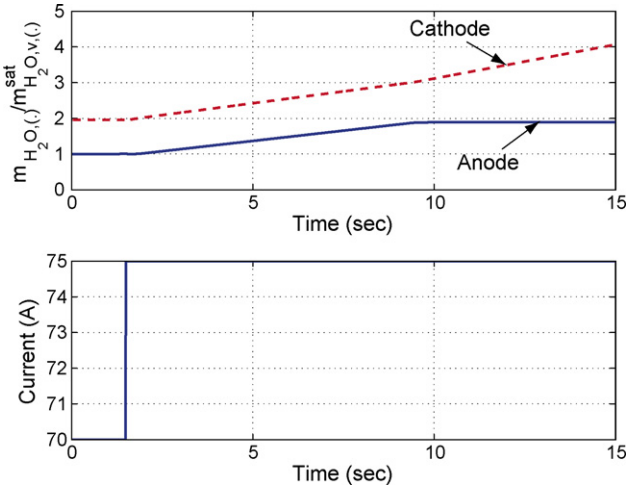

Fig. 3. Unstable water dynamics in the stack without water management: a response to a change in current drawn.

The rows in Table 1 distinguish the operating conditions in the stack based upon the water levels in the anode and the cathode electrodes. We first differentiate between sub-saturated ($m_{H_2O,(\cdot)}/m^{sat}_{H_2O,(\cdot)} < 1$) and saturated conditions ($m_{H_2O,(\cdot)}/m^{sat}_{H_2O,(\cdot)} > 1$) due to the dissimilar effects of the water vapor and liquid water on the electrode pressures. Within the saturated conditions, we also differentiate between satiated ($1 < m_{H_2O,(\cdot)}/m^{sat}_{H_2O,(\cdot)} < 3$) and soaked ($m_{H_2O,(\cdot)}/m^{sat}_{H_2O,(\cdot)} > 3$) conditions due to differences in their water content response (see Fig. 1), and hence the water diffusion through the membrane.[3] Due to space limitation, Table 1 shows only the conditions for which $a_{w,a} < a_{w,c}$, and a few of the conditions listed are elaborated here.

Consider case (i) where the water in both the anode and the cathode is only in vapor phase and a water balance is achieved in the anode and cathode. The interactions between the different states, that is, the lumped mass of cathode water, $m_{H_2O,c}$, anode water, $m_{H_2O,a}$, anode hydrogen, $m_{H_2,a}$, and cathode dry air, $m_{O_2N_2,c}$, are shown in Fig. 4. The dash-dot arrows indicate the flows in and out of the electrodes and the membrane water transport. The flows in and out of the electrodes are affected by the pressure, $p_{(\cdot)}$, and mass fraction of water vapor, $y_{v,(\cdot)}$, inside the electrodes, as seen in Eqs. (13), (21), (31) and (32). Both $p_{(\cdot)}$ and $y_{v,(\cdot)}$ depend upon the mass of water vapor and the mass of dry gas in the corresponding electrode, and this interaction is shown by the solid arrows in the figure. It is the coupling between the mass of a species in an electrode to the different inlet and exit flows that defines the stability of the equilibrium.

For example, consider a change in the stack current from its equilibrium value for a short duration that generates additional water in the cathode and disturbs the water balance. Although the stack current returns to its original value, the increase in cathode water leads to an increase in the cathode humidity. Consequently, the mass of water in the anode increases due to an increase in diffusion through the membrane. The increase in anode humidity will reduce the gradient across the membrane, and thus reduce the diffusion. Meanwhile, the increase in the anode and cathode humidities will increase the exit water flows, thereby causing the mass of water in the anode and the cathode to return to their original levels such that the exit flows balance the inlet flows. This self-balancing mechanism between the electrode humidity and the water transport across the membrane or in/out water mass flows establishes the stability of the operating points in case (i).

Now consider a case where the dynamics of both anode and cathode are unstable, for example, case (iii)-(a), where the liquid water does not leave the stack through the exit flows even

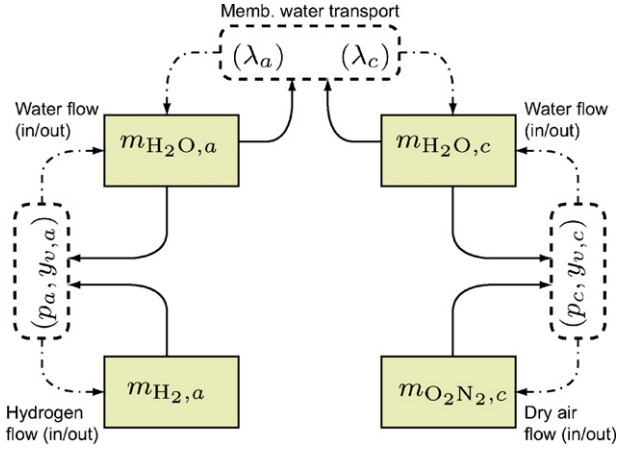

Fig. 4. Interactions between different states in the system when anode and cathode do not contain liquid water.

[3] More sub-categories can be established by considering the various possible values or models for the membrane water content. We will not elaborate on the anomalies that depend upon the definition membrane water activity.

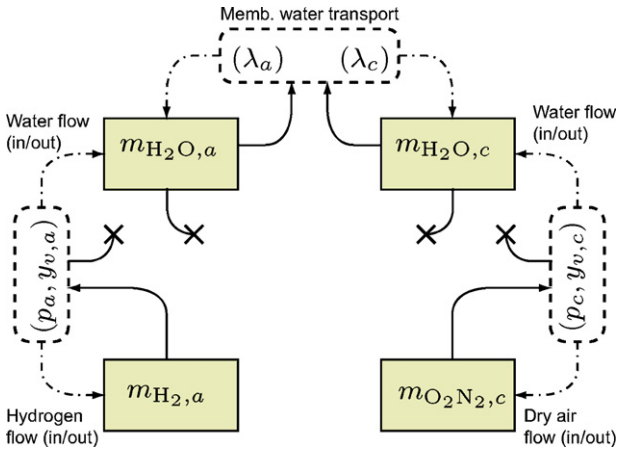

Fig. 5. Interactions between different states in the system when both anode and cathode contain liquid water and $W_{H_2O,l,out,(\cdot)} = 0$.

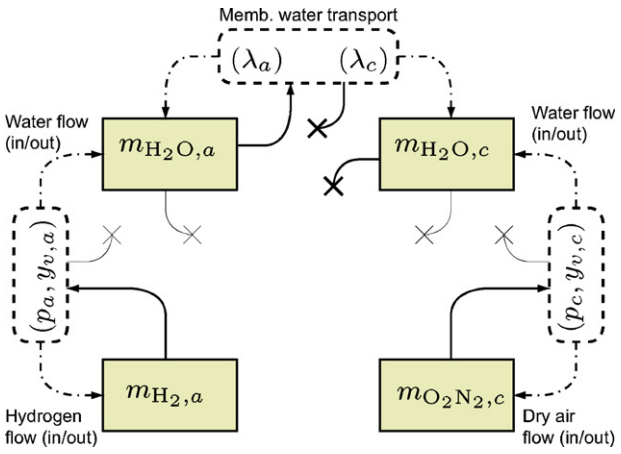

Fig. 6. Interactions between different states in the system when anode and cathode contain liquid water and the membrane water transport is independent of mass of water in cathode.

though liquid water is present in the anode and the cathode. The interaction between the various states of the system in this case is shown in Fig. 5. Both the pressure and the mass fraction of water vapor depend upon $m_{H_2O,v,(\cdot)}$, which remains constant at its maximum value $m^{sat}_{H_2O,v,(\cdot)}$. The broken lines shown in the figure imply that the mass of water in an electrode does not affect the inlet or exit flows due to their inability to affect $p_{(\cdot)}$ and $y_{v,(\cdot)}$.

In this case, a perturbation in the mass of water inside the anode or cathode does not affect $p_{(\cdot)}$ or $y_{v,(\cdot)}$, and hence, there is no change in the flows entering or leaving the stack. Note that, the total mass of water inside the stack cannot be affected by the membrane water transport. There is no stabilizing mechanism to restore the states back to their original value once they are perturbed. The mass of water in the anode and cathode electrodes may move to a different operating point depending upon the perturbation.

There are cases, such as the one shown in Fig. 3, that even though the mass of water in the cathode increases continuously due to the additional water being generated, the increase in anode water level ceases after some time (10 s in the case of Fig. 3). This phenomenon can be explained by analyzing the dynamics of an equilibrium condition in case (v)-(a), where the membrane water transport is independent of the mass of water in the cathode.

Once the cathode water content attains its maximum value, $\lambda_c = \lambda_{max}$ (see Fig. 1), the diffusion of water from cathode to anode becomes independent of the mass of water in the cathode. In Fig. 6, the broken line between $m_{H_2O,c}$ and the membrane water transport indicates that the membrane water transport does not change due to a perturbation in $m_{H_2O,c}$. The interactions between the different states of the system indicate that $m_{H_2O,c}$ does not affect the mass of water in anode. The membrane water transport depends upon $m_{H_2O,a}$, and contributes to the stability of $m_{H_2O,a}$.

The various stability results explained here using physical reasoning were validated using simulations. The results, however, can be verified analytically by using linear approximation of the system dynamics under small perturbation.

3.2. Analysis using linearization of system dynamics

Consider the fuel cell system at equilibrium with the mass of water on the cathode and anode sides as $m^*_{H_2O,c}$ and $m^*_{H_2O,a}$, respectively, the mass of hydrogen in the anode as $m^*_{H_2,a}$, and dry air in the cathode as $m^*_{O_2N_2,c}$. Assume that the states are perturbed from their equilibrium values by $x_{H_2O,c}$, $x_{H_2O,a}$, $x_{H_2,a}$ and $x_{O_2N_2,c}$, respectively, such that

$$m_{i,(\cdot)} = m^*_{i,(\cdot)} + x_{i,(\cdot)}, \tag{33}$$

where "i, $(\cdot)$" is to be replaced with "H_2O, c", "H_2O, a", "H_2, a" and "O_2N_2, c" for water in the cathode, water in the anode, hydrogen in the anode, and dry air in the cathode, respectively.

The linear approximation of the dynamics of the perturbed system with states $x_{H_2O,c}$, $x_{H_2O,a}$, $x_{H_2,a}$ and $x_{O_2N_2,c}$, is obtained by using a Taylor series expansion of Eqs. (10), (11), (27) and (29) and neglecting the higher order terms. The linearized dynamics of the perturbed system are represented using a state-space matrix notation [24] as

$$\frac{d}{dt}\begin{bmatrix} x_{H_2O,c} \\ x_{H_2O,a} \\ x_{H_2,a} \\ x_{O_2N_2,c} \end{bmatrix} = \mathcal{A}^* \begin{bmatrix} x_{H_2O,c} \\ x_{H_2O,a} \\ x_{H_2,a} \\ x_{O_2N_2,c} \end{bmatrix}, \tag{34}$$

with

$$\mathcal{A}^* = \begin{bmatrix} -\mu_c - k_{H_2O,c} & \mu_a & 0 & -k_{O_2N_2,c} \\ \mu_c & -\mu_a - k_{H_2O,a} & -k_{H_2,a} & 0 \\ 0 & -q_{H_2O,a} & -q_{H_2,a} & 0 \\ -q_{H_2O,c} & 0 & 0 & -q_{O_2N_2,c} \end{bmatrix}, \tag{35}$$

where $\mu_{(\cdot)}$, $k_{i,(\cdot)}$ and $q_{i,(\cdot)}$ are the coefficients derived from the linearization of the membrane water transport, flow of water into and out of the electrode, and gas flow into and out of the electrode, respectively. These coefficients depend upon the operating conditions associated with the equilibrium about which

the system is perturbed, and are important for establishing the stability properties of the perturbed system (34).

The coefficients related to the flows of water in the electrodes are given by

$$k_{i,(\cdot)} = -\frac{\partial W_{\mathrm{H_2O,in},(\cdot)}}{\partial m_{i,(\cdot)}} + \frac{\partial W_{\mathrm{H_2O,v,out},(\cdot)}}{\partial m_{i,(\cdot)}} + \frac{\partial W_{\mathrm{H_2O,l,out},(\cdot)}}{\partial m_{i,(\cdot)}}, \tag{36}$$

and after substituting $W_{\mathrm{H_2O},in,(\cdot)}$, $W_{\mathrm{H_2O,v,out},(\cdot)}$ and $W_{\mathrm{H_2O,l,out},(\cdot)}$ based on Eqs. (13), (22) and (25), respectively, and taking into account that the inlet pressures, $p_{\mathrm{in},(\cdot)}$, and water vapor mass fraction, $y_{\mathrm{v,in},(\cdot)}$, depend solely upon electrode inlet conditions and not on the electrode states, we get

$$\begin{aligned} k_{i,(\cdot)} &= -y_{\mathrm{v,in},(\cdot)}\tilde{k}_{\mathrm{in},(\cdot)}\left(-\frac{\partial p_{(\cdot)}}{\partial m_{i,(\cdot)}}\right) + y_{\mathrm{v},(\cdot)}\tilde{k}_{\mathrm{out},(\cdot)}\frac{\partial p_{(\cdot)}}{\partial m_{i,(\cdot)}} \\ &\quad + W_{\mathrm{out},(\cdot)}\frac{\partial y_{\mathrm{v},(\cdot)}}{\partial m_{i,(\cdot)}} + \frac{\partial W_{\mathrm{H_2O,l,out},(\cdot)}}{\partial m_{i,(\cdot)}} \\ &= \left(y_{\mathrm{v,in},(\cdot)}\tilde{k}_{\mathrm{in},(\cdot)} + y_{\mathrm{v},(\cdot)}\tilde{k}_{\mathrm{out},(\cdot)}\right)\frac{\partial p_{(\cdot)}}{\partial m_{i,(\cdot)}} \\ &\quad + W_{\mathrm{out},(\cdot)}\frac{\partial y_{\mathrm{v},(\cdot)}}{\partial m_{i,(\cdot)}} + \frac{\partial W_{\mathrm{H_2O,l,out},(\cdot)}}{\partial m_{i,(\cdot)}}. \end{aligned} \tag{37}$$

Similarly, the coefficients corresponding to the dry gas flows in the electrodes are given by

$$q_{i,(\cdot)} = -\frac{\partial W_{\mathrm{g,in},(\cdot)}}{\partial m_{i,(\cdot)}} + \frac{\partial W_{\mathrm{g,out},(\cdot)}}{\partial m_{i,(\cdot)}}, \tag{38}$$

and after using Eqs. (31) and (32) in Eq. (38) we get

$$\begin{aligned} q_{i,(\cdot)} &= -(1-y_{\mathrm{v,in},(\cdot)})\tilde{k}_{\mathrm{in},(\cdot)}\left(-\frac{\partial p_{(\cdot)}}{\partial m_{i,(\cdot)}}\right) \\ &\quad + (1-y_{\mathrm{v},(\cdot)})\tilde{k}_{\mathrm{out},(\cdot)}\frac{\partial p_{(\cdot)}}{\partial m_{i,(\cdot)}} + \left(-\frac{\partial y_{\mathrm{v},(\cdot)}}{\partial m_{i,(\cdot)}}\right)W_{\mathrm{out},(\cdot)} \\ &= \left((1-y_{\mathrm{v,in},(\cdot)})\tilde{k}_{\mathrm{in},(\cdot)} + (1-y_{\mathrm{v},(\cdot)})\tilde{k}_{\mathrm{out},(\cdot)}\right)\frac{\partial p_{(\cdot)}}{\partial m_{i,(\cdot)}} \\ &\quad - W_{\mathrm{out},(\cdot)}\frac{\partial y_{\mathrm{v},(\cdot)}}{\partial m_{i,(\cdot)}}. \end{aligned} \tag{39}$$

Eqs. (37) and (39) show that the coefficients $k_{i,(\cdot)}$ and $q_{i,(\cdot)}$ depend on how the pressures and water vapor mass fractions in the electrode, and the liquid water removed from the electrode, are affected by the accumulation of mass of species "i, $(\cdot)$", that is, $\partial p_{(\cdot)}/\partial m_{i,(\cdot)}$, $\partial y_{\mathrm{v},(\cdot)}/\partial m_{i,(\cdot)}$ and $\partial W_{\mathrm{H_2O,l,out},(\cdot)}/\partial m_{i,(\cdot)}$, respectively.

The partial derivatives of pressure and mass fraction of water vapor in an electrode with respect to the dry gases in that electrode are given by

$$\frac{\partial p_{(\cdot)}}{\partial m_{\mathrm{g},(\cdot)}} = \frac{R_{\mathrm{g},(\cdot)}T_{(\cdot)}}{\tilde{V}_{(\cdot)}} \tag{40}$$

$$, \frac{\partial y_{\mathrm{v},(\cdot)}}{\partial m_{\mathrm{g},(\cdot)}} = -\frac{y_{\mathrm{v},(\cdot)}}{m_{\mathrm{H_2O},(\cdot)} + m_{\mathrm{g},(\cdot)}} \tag{41}$$

where "g, $(\cdot)$" is replaced by "H_2, a" for hydrogen in anode and by "O_2N_2, c" for dry air in the cathode.

The partial derivatives of pressure and mass fraction of water vapor in an electrode with respect to water in that electrode are given by

$$\frac{\partial p_{(\cdot)}}{\partial m_{\mathrm{H_2O},(\cdot)}} = \frac{R_{\mathrm{H_2O}}T_{(\cdot)}}{\tilde{V}_{(\cdot)}}\frac{\partial m_{\mathrm{H_2O,v},(\cdot)}}{\partial m_{\mathrm{H_2O},(\cdot)}} \tag{42}$$

$$\frac{\partial y_{\mathrm{v},(\cdot)}}{\partial m_{\mathrm{H_2O},(\cdot)}} = \frac{1-y_{\mathrm{v},(\cdot)}}{m_{\mathrm{H_2O},(\cdot)} + m_{\mathrm{g},(\cdot)}}\frac{\partial m_{\mathrm{H_2O,v},(\cdot)}}{\partial m_{\mathrm{H_2O},(\cdot)}}, \tag{43}$$

where

$$\frac{\partial m_{\mathrm{H_2O,v},(\cdot)}}{\partial m_{\mathrm{H_2O},(\cdot)}} = \begin{cases} 1 & \text{if } m_{\mathrm{H_2O,v},(\cdot)} < m^{\mathrm{sat}}_{\mathrm{H_2O,v},(\cdot)} \\ 0 & \text{otherwise.} \end{cases} \tag{44}$$

The equation above indicates that we need to evaluate the stability of the system separately for saturated and sub-saturated conditions inside an electrode.

Finally, the coefficients related to membrane water transport are given by

$$\mu_{\mathrm{a}} = \frac{\partial W_{\mathrm{memb}}}{\partial m_{\mathrm{H_2O,a}}}, \quad \mu_{\mathrm{c}} = -\frac{\partial W_{\mathrm{memb}}}{\partial m_{\mathrm{H_2O,c}}},$$

where W_{memb} is given in Eq. (1). Note that, $\mu_{(\cdot)}$ depends upon the relation between lumped mass of water in the electrode and the corresponding water content, $\lambda_{(\cdot)}$ (see Fig. 1).

The linearized model, thus obtained, is used to determine the stability characteristics of an equilibrium condition [24], by calculating the eigenvalues of the matrix $\mathcal{A}^*$ given in Eq. (35). The eigenvalues, $\bar{s}$, are given by the solution to the characteristic equation

$$\det\{\bar{s}I_{4\times4} - \mathcal{A}^*\} = 0, \tag{45}$$

where $I_{4\times4}$ is an identity matrix. The system is indeed stable when all the four eigenvalues, $\bar{s}$, have negative real parts.

Due to the sparse nature of matrix $\mathcal{A}^*$, it is possible to rearrange the rows and columns and isolate the states associated with the stable and unstable eigenvalues. For example, in case (iii)-(a), with liquid water present in both the electrodes, $\mathcal{A}^*$ given in Eq. (35) can be simplified to

$$\mathcal{A}^* = \begin{bmatrix} -\mu_{\mathrm{c}} & \mu_{\mathrm{a}} & 0 & -k_{\mathrm{O_2N_2,c}} \\ \mu_{\mathrm{c}} & -\mu_{\mathrm{a}} & -k_{\mathrm{H_2,a}} & 0 \\ 0 & 0 & -q_{\mathrm{H_2,a}} & 0 \\ 0 & 0 & 0 & -q_{\mathrm{O_2N_2,c}} \end{bmatrix}. \tag{46}$$

This simplification is obtained by noting that $\partial p_{(\cdot)}/\partial m_{\mathrm{H_2O},(\cdot)} = 0$, $\partial y_{\mathrm{v},(\cdot)}/\partial m_{\mathrm{H_2O},(\cdot)} = 0$, and $\partial W_{\mathrm{H_2O,l,out},(\cdot)}/\partial m_{\mathrm{H_2O},(\cdot)} \equiv 0$, which leads to

$$k_{\mathrm{H_2O},(\cdot)} = 0, \quad q_{\mathrm{H_2O},(\cdot)} = 0.$$

In this case, $\mathcal{A}^*$ has an upper "block" triangular form, hence, the dynamics of the dry gases $x_{\mathrm{H_2,a}}$ and $x_{\mathrm{O_2N_2,c}}$ are independent of the water dynamics and exhibit stable behavior, since $q_{\mathrm{H_2,a}}$ and $q_{\mathrm{O_2N_2,c}}$ can be shown to be strictly positive by substituting the derivatives given by Eqs. (40) and (41) in Eq. (39).

The remaining coefficients in $\mathcal{A}^*$ correspond to the water dynamics in the two electrodes. The linear dependency between the first and second columns indicates that one of the eigenvalues is zero and the subsystem stability can only be determined

through the analysis of the nonlinear system dynamics.[4] Indeed, the nonlinear system described with the total mass of water in the two volumes by adding Eqs. (10) and (11) is governed by integrator-like dynamics. Therefore, once perturbed, the mass of water in the anode and the cathode will deviate from their equilibrium conditions in case (iii)-(a), leading to the instability conclusion.

For the case (v)-(a), the coefficient $\mu_c = 0$, since the cathode water activity exceeds 3, and hence, the membrane water transport now depends only upon mass of water in the anode, which leads to

$$\mathcal{A}^* = \begin{bmatrix} 0 & \mu_a & 0 & -k_{O_2N_2,c} \\ 0 & -\mu_a & -k_{H_2,a} & 0 \\ 0 & 0 & -q_{H_2,a} & 0 \\ 0 & 0 & 0 & -q_{O_2N_2,c} \end{bmatrix}, \quad (47)$$

with the eigenvalues of $-\mu_a$, $-q_{H_2,a}$, $-q_{O_2N_2,a}$ and 0. As discussed for case (iii)-(a), the eigenvalue at the origin is due to the integrator corresponding to the total mass of water in the stack, and is not an artifact of linearization. Meanwhile, the eigenvalue $-\mu_a$, with $\mu_a > 0$, corresponds to $x_{H_2O,a}$, indicating that the mass of water in the anode is stable even when the total mass in the stack grows unbounded.

The discussion of these few cases is not exhaustive but serves in highlighting the complexity of the water dynamic behavior that the simple two-volume model can predict. The predictions of this two-volume model are now presented under certain interesting conditions. First, the predictions without water management are discussed, and are then followed by the predictions with water management using cathode inlet humidification and anode water removal.

4. Model simulation with no water management

In this section, the steady state stack hydration characteristics without appropriate water management are predicted using the two-volume model for various fuel cell loads. The influence of the membrane diffusion parameter on these patterns is also considered in order to illustrate how the model can be tuned to match experimentally observed patterns. The prediction of flooding and drying patterns is useful in identifying the water management strategies required at different loads.

The predictions of the two-volume model depends on the choice of the inlet and exit pressures. Physically realizable inlet and exit conditions are required to predict meaningful hydration characteristics at different fuel cell loads. In this paper, the two-volume model is simulated using the stack operating conditions of a high pressure fuel cell system.

The important features of the operating conditions chosen are as follows:

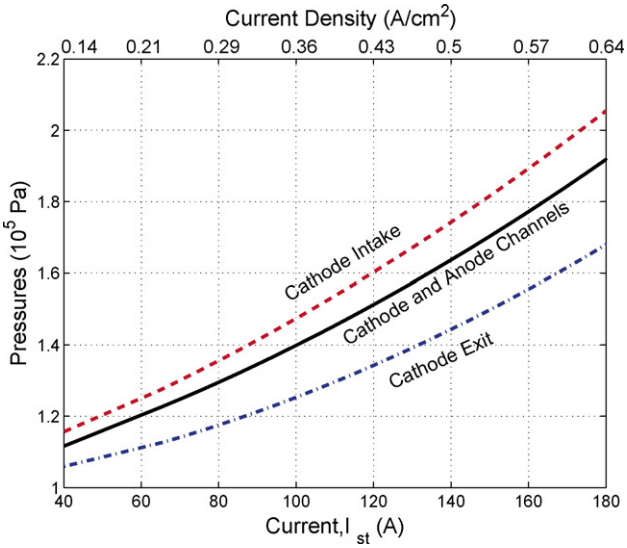

Fig. 7. Cathode inlet and the exit pressures, along with the stack pressure for oxygen excess ratio of 2.

(1) Constant temperature is assumed throughout the stack, $T_a = T_c = T_{in,a} = T_{in,c} = 353$ K.
(2) Dry hydrogen is supplied to the anode inlet, $W_{H_2O,in,a} = 0$.
(3) A dead ended anode is considered, $W_{out,a} = W_{H_2O,out,a} = 0$, where all the fuel supplied is consumed and the hydrogen excess ratio equals 1.
(4) The air flow rate is selected to provides the desired oxygen excess ratio[5] (approximately 2) required for an optimal operation of the stack [12].
(5) The air supplied to the cathode is completely humidified, $\phi_{in,c} = 1$.
(6) The cathode inlet and exit pressures are shown in Fig. 7 along with the pressure inside the stack. The stack model parameters necessary for the simulations are provided in Appendix, Table 2.
(7) Water flowing out of the cathode is only in vapor phase, $W_{H_2O,l,out,c} = 0$.

Due to the last assumption, the conditions encountered in this section belong to category (a) mentioned in Table 1.

These operating conditions are chosen as an example to demonstrate the model prediction and investigate the predicted flooding and drying steady state patterns for various loads (current drawn). In the following sections, the stack hydration characteristic, that is, the degree of flooding or drying in the anode and cathode electrodes, is quantified using the water activities in the two electrodes. Note that, the water activity, $a_{w,(\cdot)}$, is used because it is proportional to the mass of water in the electrode (see Eq. (7)). When $a_{w,(\cdot)} < 1$, the water vapor pressure in the electrode is below saturation pressure (sub-saturated condition). Conversely, when $a_{w,(\cdot)} > 1$, the water vapor pressure in the electrode has reached its saturation value and liquid water is present (saturated condition). The predicted steady state values

[4] The stability of a system cannot be decided based upon the linearization when an eigenvalue of the linearized system is at the origin.

[5] Oxygen excess ratio is the ratio of rate of oxygen supplied to the cathode to the rate at which oxygen consumed in the electrochemical process.

Table 2
Values of parameters used for simulations

Symbol	Parameter	Value
t_m	Membrane thickness	1.275×10^{-3} m
$\tilde{M}_{m,dry}$	Molecular weight of dry membrane	1.1 kg mole^{-1}
$\rho_{m,dry}$	Density of dry membrane	2×10^3 kg m^{-3}
A_{fc}	Active area of stack	0.028 m^2
n_{cells}	Number of cells in stack	381
T_{st}	Stack temperature	353 K
F	Faraday's constant	96485 Coulombs
$\tilde{V}_a$	Anode volume	0.005 m^3
$\tilde{V}_c$	Cathode volume	0.01 m^3
$\tilde{M}_{H_2O}$	Molecular weight of water	18.02×10^{-3} kg mole^{-1}
$\tilde{M}_{H_2}$	Molecular weight of hydrogen	2.016×10^{-3} kg mole^{-1}
$\tilde{M}_{O_2N_2}$	Molecular weight of dry air	29.00×10^{-3} kg mole^{-1}
α_D	Scaling on diffusion coefficient	5
$\tilde{k}_{in,c}$	Cathode inlet flow coefficient	0.36×10^{-5} kg s^{-1} Pa^{-1}
$\tilde{k}_{out,c}$	Cathode outlet flow coefficient	0.22×10^{-5} kg s^{-1} Pa^{-1}

of anode and cathode water activities, $a_{w,c}$ and $a_{w,a}$, and their corresponding water contents, λ_c and λ_a, respectively, are shown in Fig. 8 for different stack currents, I_{st}. The absolute value of stack current is indicated by the lower horizontal axis while the upper axis is used to denote the corresponding current density, $i_{st} = I_{st}/A_{fc}$.

At all current densities, the electro-osmotic drag creates a water flow from anode to the cathode, which depletes the mass water in the anode while increasing the water in cathode. This creates a gradient between the water activities on the anode and cathode sides of the membrane. The gradient causes a back-diffusion from the cathode to the anode, whose magnitude depends upon $\lambda_c - \lambda_a$, the difference in the water contents on both sides of the membrane (see Eq. (3)). For the dead ended anode with dry anode inlet flow (i.e., $W_{H_2O,in,a} = W_{H_2O,out,a} = 0$) considered here, anode side water equilibrium, $dm_{H_2O,a}/dt = 0$, is attained when $\lambda_c - \lambda_a$ is such that the back diffusion balances the electro-osmotic drag, that is, $W_{memb} = 0$. Therefore, for anode water to be at equilibrium, the conditions $\lambda_a < \lambda_c$, and correspondingly, $a_{w,a} < a_{w,c}$, must be satisfied as seen in Fig. 8.

At the low current densities ($i_{st} < 0.2$ A cm^{-2} for the fuel cell model considered here), the cathode inlet flow humidification and water generated are inadequate to keep the cathode completely humidified, and hence, at steady state the cathode is sub-saturated, that is, $a_{w,c} < 1$. The mass of water inside the anode also reaches steady state such that $a_{w,a} < a_{w,c} < 1$. This condition belongs to case (i)-(a), and as discussed in Section 3, it corresponds to water equilibria with stable dynamic behavior. The physical mechanism responsible for an increase in cathode humidity with stack current is as follows. The rate of water generation increases with stack current, and is accompanied by an increase in mass of water inside the cathode, $m_{H_2O,c}$, and the water activity, $a_{w,c}$, for given oxygen excess ratio. The increase in $m_{H_2O,c}$ causes a higher mass fraction of vapor in the gas leaving the cathode and allows sufficient increase in $W_{H_2O,out,c}$ to achieve water balance in the cathode, $dm_{H_2O,c}/dt = 0$.

Once $a_{w,c} = 1$, that is, $m_{H_2O,c} = m^{sat}_{H_2O,v,c}$, additional increase in mass of water in the cathode does not affect $W_{H_2O,out,c}$ for a given flow rate of dry gas, due to the assumption that only water vapor is carried out of the electrode. Above $i_{st} = 0.2$ A cm^{-2}, the water removed from a saturated cathode is less than the total water entering the electrode through water generation and humidification of cathode inlet flow. Therefore, $dm_{H_2O,c}/dt > 0$, and excess water accumulates as liquid in the cathode while a part of water is transferred to the anode due to back diffusion through the membrane. The condition at $i_{st} = 0.2$ A cm^{-2} corresponds to an unstable equilibrium of case (iii)-(a), and $m_{H_2O,c}$ and $m_{H_2O,a}$ increase with time due to an imbalance between the water supply and removal from the stack. This is shown in Fig. 8(a) with the vertical line at $I_{st} = 60A$ ($i_{st} = 0.2$ A cm^{-2}).

If the fuel cell operates long enough at $i_{st} = 0.2$ A cm^{-2}, the mass of water in the cathode exceeds a value such that, $a_{w,c} \geq 3$, in which case the cathode water content saturates at 16.8 as shown in Fig. 1. This condition corresponds to case (v)-(a), in which the membrane water transport is independent of the mass of water in cathode, and only depends on the anode water con-

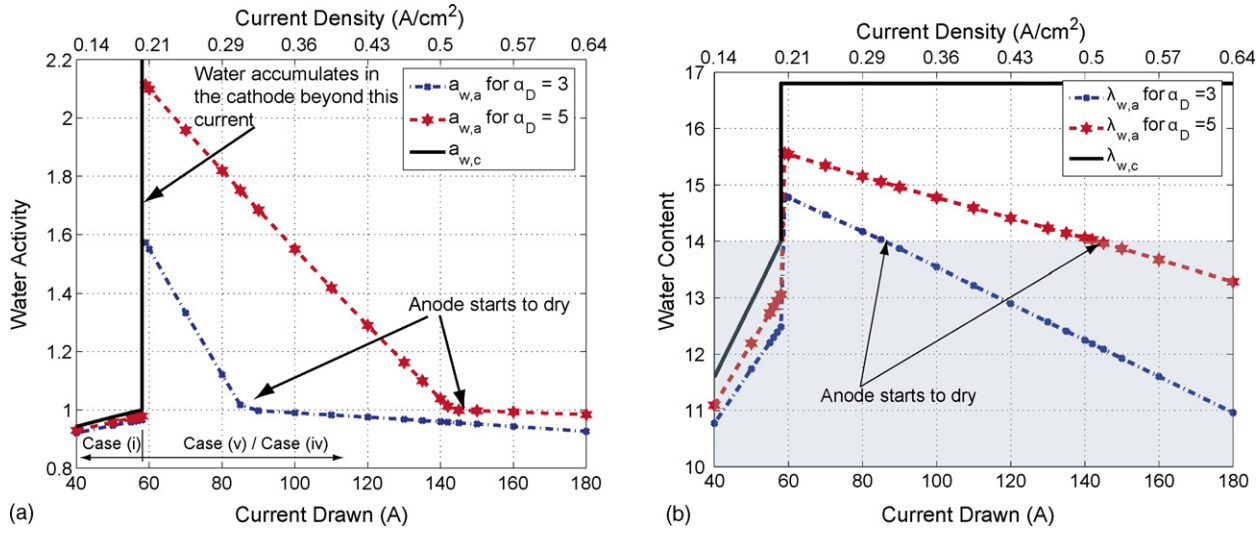

Fig. 8. The predicted anode and cathode water activities and water contents at steady state without water management. The cathode conditions are shown by the solid black lines. The anode side conditions depend upon the membrane characteristics and are shown for two different diffusion coefficients.

tent. This dependence provides the stabilizing factor for $a_{w,a}$. The mass of water in the anode equilibrates such that the water diffusion through the membrane from cathode to anode is balanced by the electro-osmotic drag. As shown in Fig. 8, the discontinuity in $a_{w,a}$, is a direct consequence of the jump in cathode water content (from 14 to 16.8) at the current density where the stack begins to flood.

The increase in stack current causes a higher electro-osmotic drag which tends to reduce $a_{w,a}$ and increase $a_{w,c}$. The resulting increase in the difference between the anode and cathode side membrane water contents, $\lambda_c - \lambda_a$, provides sufficient diffusion to balance the electro-osmotic drag, so that $W_{memb} = 0$. Note here that, below $i_{st} = 0.2\,A\,cm^{-2}$, although $\lambda_c - \lambda_a$ increases with stack current, the increase in λ_c leads to an increase in λ_a, and hence $a_{w,a}$, with current. Above $i_{st} = 0.2\,A\,cm^{-2}$, λ_c is saturated at 16.8, and hence, increase in $\lambda_c - \lambda_a$ is caused by the decrease in $a_{w,a}$, and this decrease in $a_{w,a}$ continues for higher current densities ($i_{st} > 0.2\,A\,cm^{-2}$).

At sufficiently high stack current densities, the membrane water transport is inadequate to keep the anode completely humidified, and hence, $a_{w,a} < 1$, leading to dehydration of the anode side of the membrane. The slope of the $a_{w,a}$ versus I_{st}, as well as the current densities where the anode starts to dry, depend upon the membrane water transport properties, namely, the coefficients for diffusion and the electro-osmotic drag. Experimental data of the current densities at which we observe transitions from sub-saturated to saturated conditions [25], and back from saturated to sub-saturated conditions in the anode can be used to tune the membrane model and especially the coefficients α_D and n_d. For the rest of the paper, $\alpha_D = 5$ is used such that the anode returns to sub-saturated conditions around 150A ($i_{st} = 0.54\,A\,cm^{-2}$).

The membrane model developed in this paper allows the prediction of the onset of anode flooding due to cathode flooding at low current densities and the anode drying at high current densities [10]. These phenomena have been observed experimentally using various visualization techniques [25,2]. The flooding and water accumulation inside the stack further can be prevented by controlling flows entering and/or leaving the stack, as discussed in subsequent section.

5. Stack water management

The stack hydration characteristics predicted by the two-volume model are discussed in this section for two different water management strategies. One is using only cathode inlet humidity to achieve water management requirements, while the other is using maximum anode water removal plus appropriate cathode inlet humidification.

The purpose of these water management strategies is to avoid water accumulation while maintaining saturated conditions in the anode and cathode electrodes, that is, $a_{w,c}, a_{w,a} \geq 1$. This constraint avoids sub-saturated conditions on the sides of the membrane that can decrease the stack performance [17]. Meanwhile, least amount of liquid water in the anode and cathode is desired, since the presence of excessive liquid water inside the stack may block the reactant supply to the electrodes and affect the stack voltage. Considering that both sides of the membrane need to be 100% humidified, and $a_{w,a} < a_{w,c}$, this is achieved with $a_{w,a} = 1$.

Without active water management, there is no guarantee for water balance and the water in the anode and cathode electrodes could deplete or accumulate, such as the case shown in Fig. 3. A control volume analysis of the fuel cell stack renders the rate of water accumulation inside the stack, $W_{H_2O,stack}$, as

$$W_{H_2O,stack} = W_{H_2O,gen} + W_{H_2O,in,c} - W_{H_2O,out,c} - W_{rem,a}, \tag{48}$$

where for the ease of notation we define the net water removed from the anode side, $W_{rem,a}$, as

$$W_{rem,a} = W_{H_2O,out,a} - W_{H_2O,in,a}. \tag{49}$$

Thus, the water management objective is to prevent water accumulation inside the stack by maintaining $W_{H_2O,stack} = 0$ and to regulate $a_{w,a} = 1$. These water management requirements should be met using appropriate cathode inlet humidification along with water removal from anode side, subject to the constraint that the air flow is controlled to meet the oxygen excess ratio.

5.1. Water management using variable cathode inlet flow humidity

The first strategy uses only cathode inlet humidity to control the rate of water entering the cathode such that the water management requirements are met without anode water removal, (that is, $W_{rem,a} = 0$). The desired cathode inlet water flow, $W^{des}_{H_2O,in,c}$, to achieve $W_{H_2O,stack} = 0$ is obtained by rearranging Eq. (48) as

$$W^{des}_{H_2O,in,c} = W^{sat}_{H_2O,out,c} - W_{H_2O,gen}, \tag{50}$$

where $W_{H_2O,out,c}$ is replaced by $W^{sat}_{H_2O,out,c}$, the water removed out of the cathode under saturated conditions ($a_{w,c} \geq 1$). Note here that, we impose condition (50) to find the requirements for achieving a fully humidified cathode.

In Fig. 9(a), $W^{sat}_{H_2O,out,c}$ is shown by the dashed line while $W_{H_2O,gen}$ is shown by the dash-dot line for different stack currents. The corresponding $W^{des}_{H_2O,in,c}$ is given by the solid line in Fig. 9(b). In the figure, the dashed line represents $W^{sat}_{H_2O,in,c}$, the maximum cathode inlet water flow in vapor phase that can be attained for a given dry gas flow rate (oxygen excess ratio). Since $W^{sat}_{H_2O,in,c}$, corresponds to 100% humidified cathode inlet flow, the desired cathode inlet humidity, $\phi^{des}_{in,c}$, is then given by

$$\phi^{des}_{in,c} = \min\left\{\frac{W^{des}_{H_2O,in,c}}{W^{sat}_{H_2O,in,c}},\quad 1\right\}, \tag{51}$$

which is shown in Fig. 10.

Clearly at low current densities ($i_{st} < 0.2\,A\,cm^{-2}$), the desired water supply to keep the stack humidified cannot be met even with 100% humidification. Due to inadequate water supply to sustain $a_{w,c} = 1$ at steady state, the cathode and anode electrodes will be sub-saturated as seen in Fig. 8. In this case, the amount of water vapor supplied to the cathode can be increased

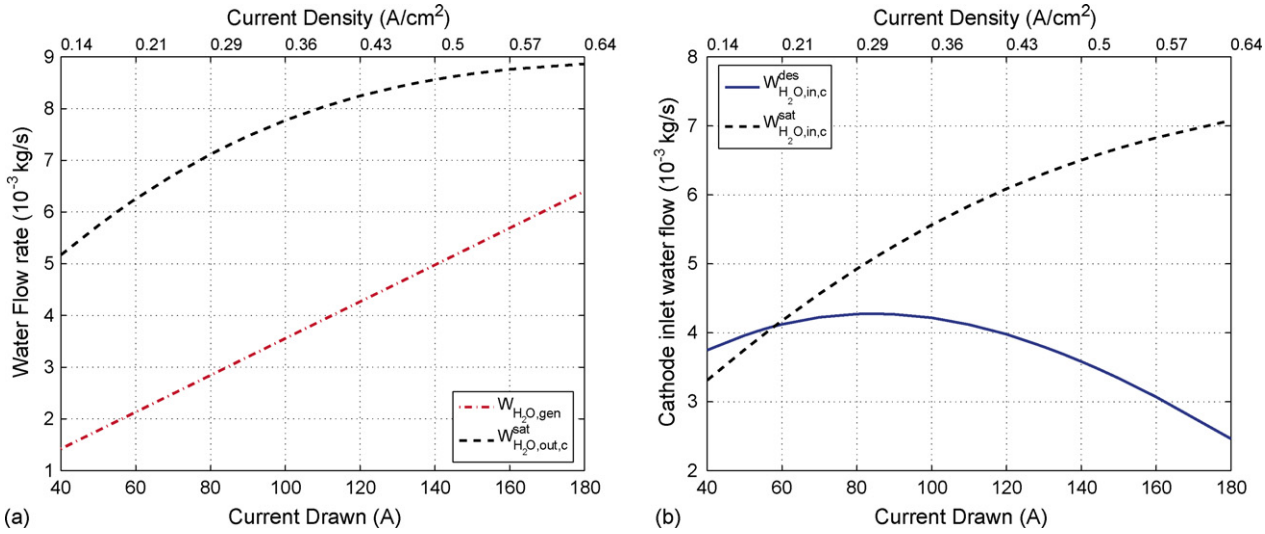

Fig. 9. Flows that influence the water management requirements, and hence, the desired cathode water inlet flow rates required for stack water balance at various current densities.

by modifying the oxygen excess ratio, which is beyond the scope of this paper. As the current density increases, the increase in water generated through the electrochemical reaction reduces the humidity requirement for the cathode inlet flow, as shown in Fig. 10.

Fig. 11(a) shows the steady state cathode and anode water activities obtained by using this desired cathode inlet humidification, and regulating anode water activity at 1. The cathode inlet humidity is set using a feedforward map from the current as shown in Fig. 11(b) to provide the water balance. The feedforward map, however, will not guarantee that the desired water activities are attained, since the desired equilibrium conditions belonging to case (iii)-(a) are unstable. The desired anode water activity is obtained by using a feedback control scheme, such as the one shown in Fig. 11(b).

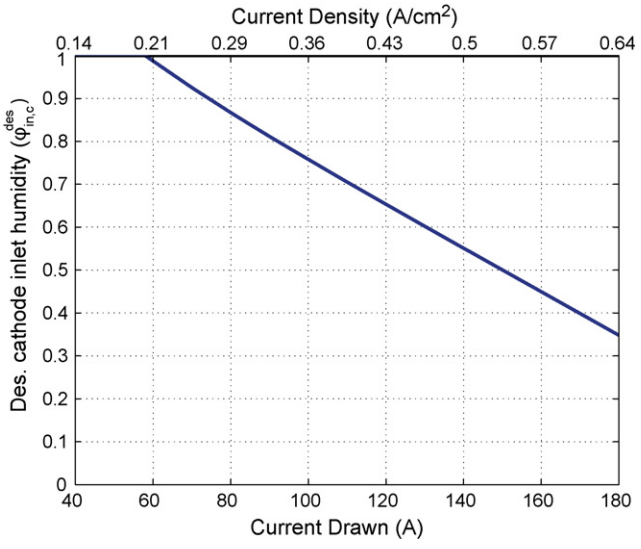

Fig. 10. Desired cathode inlet flow humidification to maintain $W_{H_2,O,stack} = 0$ with no water removal from anode side.

As the current density increases, the higher difference required at steady state between λ_c and λ_a is achieved with an increase in $a_{w,c}$. Since increasing $a_{w,c}$ above 3 does not increase the diffusion, therefore, beyond $i_{st} = 0.54\,A\,cm^{-2}$ the anode cannot be kept completely humidified due to the limitations imposed by the membrane water transport characteristics, and maintaining a water balance will result in $a_{w,a} < 1$. In this case, the maximum anode humidity can be achieved by maintaining $a_{w,c} = 3$.

Although controlling the cathode inlet humidity could clearly achieve the stated requirements between $i_{st} = 0.2\,A\,cm^{-2}$ and $i_{st} = 0.54\,A\,cm^{-2}$, lowering cathode inlet humidity is not always desirable. First, controlling the inlet humidity fast and accurately is limited by the slow temperature dynamics of the humidifier [26]. Second, reducing the cathode inlet humidity can dry the cells closer to the air inlet manifold and thus increase cell to cell variations.

Alternatively, anode water removal can be employed in coordination with cathode inlet humidification to achieve the desired water management requirements, as investigated in the next section.

5.2. Water management using anode water removal with variable cathode inlet humidity

The water management requirement delineated at the beginning of this section can also be achieved using water removal from the anode [15]. If anode water removal alone is inadequate to satisfy the water management requirements, only then the cathode inlet flow humidity is reduced below 100% to complement the anode water removal. The water removal can be obtained using excess hydrogen fuel, which is typically desired in order to achieve adequate fuel supply at the downstream end of the anode electrode. If this excess fuel is being recirculated [27,14], then a water removal device can be used to remove the water from the anode exit stream before the recirculated flow is introduced in the anode inlet side of the fuel cell system.

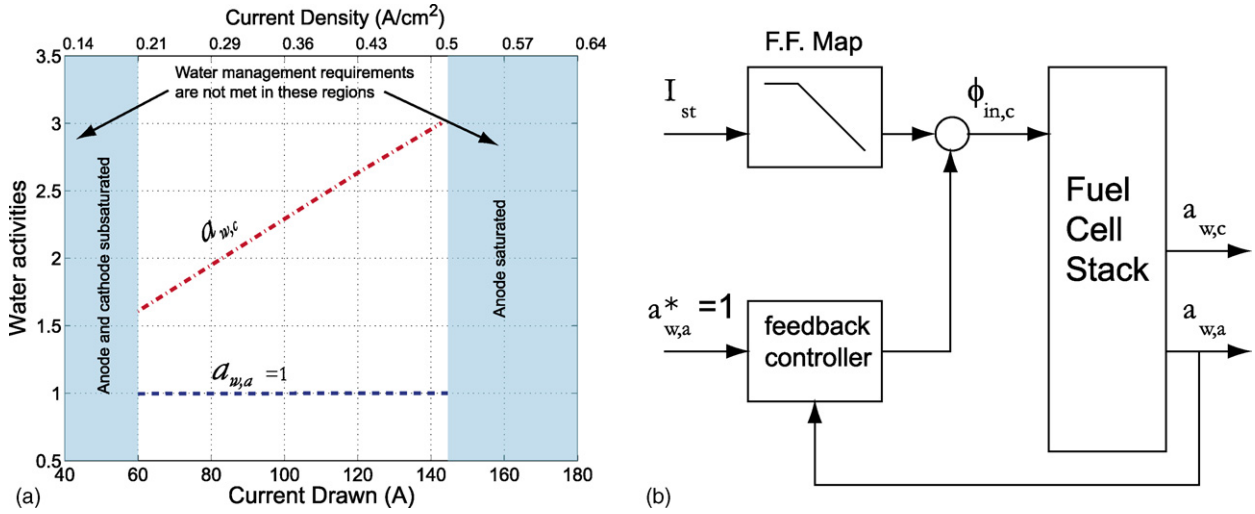

Fig. 11. Anode and cathode steady state response using desired cathode inlet humidification at steady state to maintain $W_{H_2,O,stack} = 0$ is shown in (a). In (b), the control architecture used to regulate the anode water activity to 1 is shown.

The required anode water removal leading to $W_{H_2O,stack} = 0$, can be expressed as

$$W^{req}_{rem,a} = W_{H_2O,gen} + W_{H_2O,in,c} - W^{sat}_{H_2O,out,c}, \quad (52)$$

by rearranging Eq. (48), where $W^{sat}_{H_2O,out,c}$ represents water removed from the cathode when the cathode is saturated, a condition that is satisfied for $i_{st} > 0.2\,A\,cm^{-2}$ (see Fig. 8).

Fig. 12 shows the anode water removal required for different cathode inlet flow humidities. The maximum anode water removal is required with saturated cathode inlet flow, that is, when $W_{H_2O,in,c} = W^{sat}_{H_2O,in,c}$. Despite saturated cathode inlet flow, a negative anode water removal is required when $i_{st} < 0.2\,A\,cm^{-2}$, since the water generated and supplied are not enough to maintain saturated condition in the cathode, as shown in Fig. 8. Instead of anode water removal, the anode inlet flow should be humidified when $W^{req}_{rem,a} < 0$, to maintain a saturated stack.

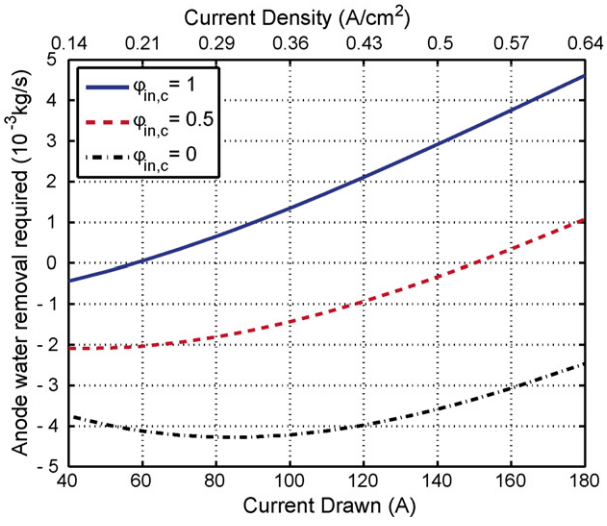

Fig. 12. Anode water removal required to maintain $W_{H_2,O,stack} = 0$, for different humidities of cathode inlet flow. For conditions with $W_{rem,a} < 0$, additional humidification is required to keep the both sides of the membrane saturated.

We now establish the feasibility of the anode water removal, that is, for which stack currents is it possible to remove all this water from the anode. The anode water removal capacity is limited by the amount of water transported through the membrane. For $a_{w,a} \geq 1$, the maximum water transported from the cathode to the anode is achieved with the maximum difference in water contents on the cathode and anode sides. This maximum water transport from cathode to anode, W^{max}_{memb}, is achieved when $a_{w,a} = 1$ with $\lambda_a = 14$, and $\lambda_c = \lambda_{max}$, for which $a_{w,c} \geq 3$.

A thinner or a more diffusive membrane can provide a greater W^{max}_{memb}. In Fig. 13(a), W^{max}_{memb} corresponding to $\alpha_D = 5$ is shown by the dashed line. The decrease in W^{max}_{memb} with increase in current drawn is due to the increase of water transferred from the anode to the cathode as the result of increased electro-osmotic drag. In the same figure, $W^{req}_{rem,a}$, the anode water removal required to prevent the fuel cell stack flooding with 100% humidified cathode inlet flow, is shown by the dash-dot line in Fig. 13(a).

Above $i_{st} = 0.43\,A\,cm^{-2}$, the rate at which the water accumulates in the fuel cell stack is higher than the maximum rate at which water is transferred to the anode side, thereby limiting the authority of anode water removal. Based upon Fig. 13(a), the desired anode water removal, $W^{des}_{rem,a}$, to prevent anode flooding or drying is given by the minimum of the two values between the dash-dot and the dashed lines, that is,

$$W^{des}_{rem,a} = \min\left\{W^{req}_{rem,a}, W^{max}_{memb}\right\}. \quad (53)$$

This $W^{des}_{rem,a}$ meets the anode water management requirement, but will not be able to meet the water removal requirement for the stack for $i_{st} > 0.43\,A\,cm^{-2}$. In this case, the desired cathode inlet flow humidity, $\phi^{des}_{in,c}$, necessary to achieve $W_{H_2O,stack} = 0$, is given by

$$\phi^{des}_{in,c} = \min\left\{\frac{W^{des}_{rem,a} + W^{sat}_{H_2O,out,c} - W_{H_2O,gen}}{W^{sat}_{H_2O,in,c}}, \quad 1\right\}. \quad (54)$$

The desired cathode inlet flow humidity decreases with increase in i_{st} beyond $0.43\,A\,cm^{-2}$, as shown in Fig. 13(b). For com-

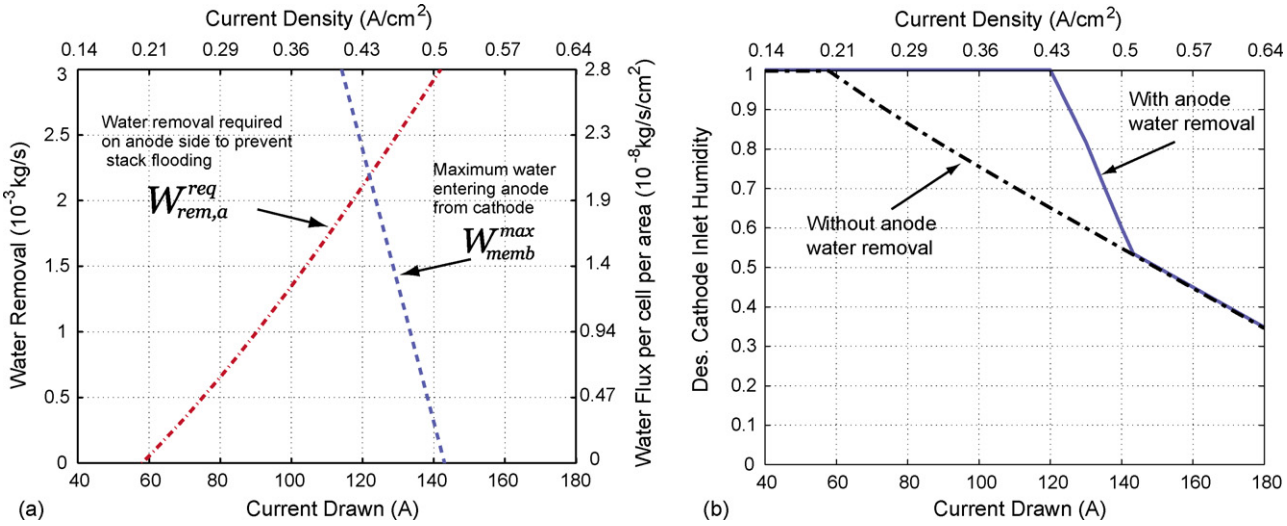

Fig. 13. Water management using anode water removal and cathode inlet flow humidification. In (a), the desired anode water removal is the minimum of dash-dot line, representing $W^{\text{req}}_{\text{rem,a}}$, and dashed line, representing $W^{\text{max}}_{\text{memb}}$.

parison, the desired cathode inlet humidity for the system without anode water removal is also included in Fig. 13(b) as the dash-dot line. The use of anode water removal allows cathode inlet air to be fully humidified in a wider current density range (0–0.43 A cm^{-2}), compared to the system without anode water removal (0–0.2 A cm^{-2}).

Beyond $i_{\text{st}} = 0.54\,\text{A cm}^{-2}$, the maximum membrane water transport from cathode to anode is negative when the anode is 100% humidified, hence, even with $W^{\text{des}}_{\text{rem,a}} = 0$ the anode will be sub-saturated ($a_{\text{w,a}} < 1$). With $W^{\text{des}}_{\text{rem,a}} = 0$, water management strategy similar to that discussed in Section 5.1 should be used, in which, only cathode inlet flow humidification is used to mitigate stack flooding. As seen in Fig. 13(b), the desired cathode inlet humidity is identical for both cases when $i_{\text{st}} > 0.54\,\text{A cm}^{-2}$. The humidification of anode inlet flow is then necessary to maintain $a_{\text{w,a}} = 1$.

Fig. 14(a) shows the cathode water activity obtained by using desired anode water removal and desired cathode inlet humidification. As discussed earlier the anode and cathode are saturated, and hence, have unstable water equilibria in the stack. For $0.2\,\text{A cm}^{-2} > i_{\text{st}} > 0.43\,\text{A cm}^{-2}$ the equilibrium conditions belong to case (iii)-(a) discussed in Section 3, the anode water removal is controlled using a feedback controller to maintain the $a_{\text{w,a}} = 1$, as shown in Fig. 14. With $0.43\,\text{A cm}^{-2} > i_{\text{st}} > 0.54\,\text{A cm}^{-2}$, however, the desired equilibrium conditions belong to case (v)-(a) where the dynamics of anode and cathode are decoupled (see Fig. 6). Now, the mass of water in the cathode has unstable equilibria, and hence, the cathode water activity needs to be regulated when $i_{\text{st}} > 0.43\,\text{A cm}^{-2}$.

Compared to the strategy with only variable cathode inlet humidity, this strategy results in a higher steady state $a_{\text{w,c}}$ between $i_{\text{st}} = 0.20\,\text{A cm}^{-2}$ and $i_{\text{st}} = 0.54\,\text{A cm}^{-2}$, in order to support a higher diffusion through the membrane. Higher diffusion is required in this case to balance both electro-osmotic drag and anode water removal at steady state, as seen from Eq. (10). The advantage, however, is that the cathode inlet humidity can be

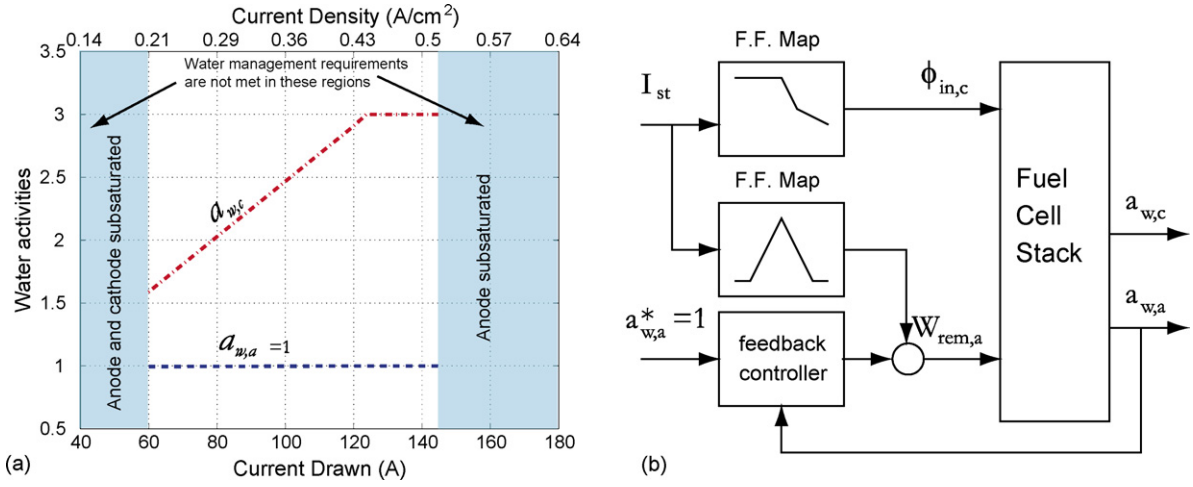

Fig. 14. Anode and cathode steady state response using desired anode water removal along with cathode inlet humidification at steady state to maintain $W_{\text{H}_2\text{O,stack}} = 0$ is shown in (a). The control architecture used to regulate anode water activity to 1 for $0.2\,\text{A cm}^{-2} < i_{\text{st}} < 0.43\,\text{A cm}^{-2}$ is shown in (b).

higher to avoid local drying at the cathode inlet. In addition, this system relies less on the cathode inlet humidity control, which often presents a challenge given the slow dynamics of the humidifier. It should be noted that even with anode water removal, the water management requirements can not be met for stack current densities below 0.2 A cm^{-2} or above 0.54 A cm^{-2}. In fact, this strategy results in the same anode and cathode activities as using cathode inlet humidification only.

5.3. Summary of water management strategies

The water management strategy discussed above maintains a saturated anode using maximum possible anode water removal and complementing it with appropriate cathode inlet humidity. This strategy is not unique. For example, the water management requirements can also be met by using a lower cathode inlet humidification accompanied by a lower anode water removal.

The use of different combinations of anode water removal and cathode inlet humidity is summarized pictorially in Fig. 15, where each circle or square denotes a unit flow rate of water. The squares shown in the figure should be ignored in the absence of anode water removal. With only variable cathode inlet humidity, the sum of the circles shown in the first and second column ($W_{H_2O,gen}$ and $W_{H_2O,in,c}$), should equal the solid circles in the third column ($W_{H_2O,out,c}$) in order to achieve water balance. An excess of solid circles in the third column results in a subsaturated cathode due to excess cathode water removal.

The squares in the second column ($W_{H_2O,in,c}$) and fourth column ($W_{rem,a}$) should be included when using anode water removal. In this case, the sum of circles and squares in the first two columns should equal the sum of circles and squares in the last two columns. Here, the additional cathode inlet humidification is balanced by providing appropriate anode water removal.

Besides water balance, other factors may also constrain the desired anode water removal and cathode inlet humidity. For example, the excess hydrogen supply on the anode side, essential for anode water removal, may be subject to constraints of specific recirculation device used. On the other hand, a consequence of combining anode water removal with higher cathode inlet humidification is the increase in cathode flooding when the anode humidity is regulated at 100%. These constraints need to be considered in specifying the requirements for anode water removal and cathode inlet humidity [16].

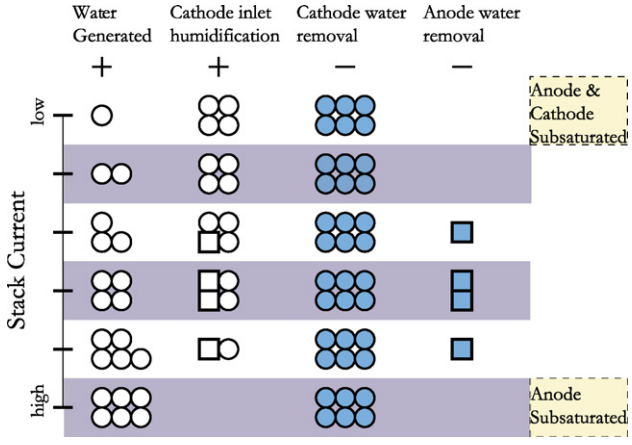

Fig. 15. Summary of the different water management strategies required to avoid fuel cell stack flooding and specifically maintaining anode humidity at 1.

6. Conclusion

A simple fuel cell stack hydration model is presented in this paper and is used for water management studies. The model predicts anode flooding at low to medium loads once the cathode floods. The amount of anode flooding reduces with increase in current density and the anode exhibits drying at high current densities while the cathode is flooding. We show how the predicted pattern is influenced by model coefficients such as the membrane water diffusion. This coefficient can be used to calibrate the model and match experimentally observed patterns of electrode flooding as a function of the current drawn from the cell.

The water management strategy necessary to maintain a humidified anode without the presence of any liquid in the anode is systematically analyzed. The feasibility of meeting the water management requirements with a combination of anode water removal and cathode inlet humidification is discussed for a high pressure fuel cell system without anode inlet flow humidification. The water removal requirement increases with stack current, however, the effectiveness of removing water from the anode side is limited by the water transport capability of the membrane which is restricted at higher current densities due to the large electro-osmotic drag. Therefore, at high current levels, reduction in cathode inlet humidification is necessary to meet the water management requirements.

In addition to selecting the set-points for anode water removal and cathode inlet humidification, a feedback controller is necessary to regulate the system hydration at its desired levels. The need for a feedback controller is demonstrated by performing a stability analysis for the system under different operating conditions, and showing a lack of self stabilizing characteristic of the system at selected operating conditions. The stability analysis results depend upon the nature of interaction between the liquid water inside the electrodes and the water leaving the electrodes.

Acknowledgement

The work reported in this paper is supported by Ford Motor Company through the University Research Program.

References

[1] T.E. Springer, T.A. Zawodzinski, S. Gottesfeld, J. Electrochem. Soc. 138 (8) (1991) 2334–2342.
[2] D. Spernjak, S. Advani, A.K. Prasad, Experimental investigation of liquid water formation and transport in a transparent single-serpentine PEM fuel cell, in: Fourth International Conference on Fuel Cell Science, Engineering and Technology (FUELCELL2006–97271), June 2006.
[3] F.N. Büchi, G.G. Scherer, J. Electrochem. Soc. 148 (3) (2001) A183–A188.
[4] M. Eikerling, A.A. Kornyshev, A.R. Kucernak, Phys. Today (2006) 38–44.
[5] L. Ma, D.B. Ingham, M. Pourkashanian, E. Carcadea, J. Fuel Cell Sci. Technol. 2 (4) (2005) 246–257.
[6] Y. Wang, C.Y. Wang, J. Power Sources 153 (1) (2006) 130–135.

[7] F. Barbir, H. Görgün, X. Wang, J. Power Sources 141 (1) (2005) 96–101.
[8] J.T. Pukrushpan, H. Peng, A.G. Stefanopoulou, Trans. ASME 126 (1) (2004) 14–25.
[9] A.B. Geiger, A. Tsukada, E. Lehmann, P. Vontobel, A. Wokaun, G.G. Scherer, Fuel Cells 2 (2) (2002) 92–98.
[10] P. Sridhar, R. Perumal, N. Rajalakshmi, M. Raja, K.S. Dhathathreyan, J. Power Sources 101 (1) (2001) 72–78.
[11] S. Dutta, S. Shimpalee, J.W. Van Zee, J. Appl. Electrochem. 30 (2) (2000) 135–146.
[12] J.T. Pukrushpan, A.G. Stefanopoulou, H. Peng, Fuel cell power systems: principles, modeling, analysis and feedback design, Advances in Industrial Control, Springer-Verlag, Telos, 2004.
[13] P. Rodatz, O. Garcia, L. Guzzella, F. Büchi, M. Bärtschi, A. Tsukada, P. Dietrich, R. Kotz, G. Scherer, A. Wokaun, Design and integration challenges for a fuel cell hybrid electric sport utility vehicle, SAE Congress (2003–01-0418), March 2003.
[14] P. Rodatz, A. Tsukada, M. Mladek, L. Guzzella, Efficiency improvements by pulsed hydrogen supply in PEM fuel cell systems, in: Proceedings of the 15th IFAC Triennial World Congress, 2002.
[15] H.H. Voss, D.P. Wilkinson, P.G. Pickup, M.C. Johnson, V. Basura, Electrochim. Acta 40 (3) (1995) 321–328.
[16] D.M. Bernardi, J. Electrochem. Soc. 137 (11) (1990) 3344–3350.
[17] F.N. Büchi, S. Srinivasan, J. Electrochem. Soc. 144 (8) (1997) 2767–2772.
[18] T.V. Nguyen, R.E. White, J. Electrochem. Soc. 140 (8) (1993) 2178–2186.
[19] U. Pasaogullari, C.Y. Wang, J. Electrochem. Soc. 152 (2) (2005) 245–251.
[20] J.S. Yi, T.V. Nguyen, J. Electrochem. Soc. 145 (4) (1998) 1149–1159.
[21] D.A. McKay, W.T. Ott, A.G. Stefanopoulou, Modeling, parameter identification, and validation of reactant and water dynamics for a fuel cell stack, in: Proceedings of IMECE–2005 (IMECE2005–81484), November 2005.
[22] A.Z. Weber, J. Newman, J. Electrochem. Soc. 151 (2) (2004) 326–339.
[23] F.Y. Zhang, X.G. Yang, C.Y. Wang, J. Electrochem. Soc. 153 (2) (2006) A225–A232.
[24] G.F. Franklin, J.D. Powell, A.E. Naeini, Feedback Control of Dynamic Systems, fifth ed., Prentice Hall, Upper Saddle River, NJ, 2005, ISBN: 0131499300.
[25] K. Tüber, D. Pocza, C. Hebling, J. Power Sources 124 (2) (2003) 403–414.
[26] D. Chen, H. Peng, Analysis of non-minimum phase behavior of PEM fuel cell membrane humidification systems, in: Proceedings of American Control Conference, June 2005, pp. 3853–3858.
[27] A.Y. Karnik, J. Sun, J.H. Buckland, Control analysis of ejector based fuel cell anode recirculation system, in: Proceedings of American Control Conference, June 2006.